Complete, rapid and reversible regulation of the motility of a nano-biomolecular machine using an osmolyte trimethylamine-*N*-oxide

Tasrina Munmun,[1,#] Arif Md. Rashedul Kabir,[2,#] Kazuki Sada,[1,2] and Akira Kakugo[1,2,]*

[1]Graduate School of Chemical science and Engineering, Hokkaido University, Sapporo 060-0810, Japan.

[2]Faculty of Science, Hokkaido University, Sapporo 060-0810, Japan.

*Corresponding author

E-mail: kakugo@sci.hokudai.ac.jp

[#]These authors contributed equally to this work.

Abstract

Nanoscale transportation in engineered environments is critical towards designing efficient and smart hybrid bio-nanodevices. Biomolecular motors, the smallest natural machines, are promising as actuators as well as sensors in hybrid nanodevices and hold enormous potentials in nanoscale transportation. Highly specific regulation of the functions of biomolecular motors is the key to control such integrated nanodevices. We present a simple method to regulate the activity of a biomolecular motor system, microtubule (MT)-kinesin by using a natural osmolyte trimethylamine-*N*-oxide (TMAO). Motility of kinesin-driven MTs in an in vitro gliding assay is regulated over a broad spectrum by using TMAO in a concentration dependent manner. The regulation of MT motility is rapid, reversible and repeatable over multiple cycles. Interestingly, the motility of MTs can be completely turned off using TMAO of a relatively high concentration. The halted motility of MTs is fully restored upon elimination of TMAO. Repeated cycles of TMAO addition and removal enable cyclical inhibition and restoration of the motility of MTs. These results demonstrate an ability to control nanoscale motion of a biomolecular motor in an artificial environment. This work facilitates further tunability over functions of biomolecular motors, which in turn will foster their nanotechnological applications, such as in nano-transportation.

Key words: Biomolecular motor, Kinesin, Microtubule, On-off switching, Osmolyte, TMAO.

1. Introduction

Active transport systems in living organisms ensure directed, non-equilibrium transportation of materials to meet their physiological needs and enable their adaptation to any change in their environment [1,2]. Many cellular processes such as cell division, intracellular transportation of vesicles, organelles and signaling molecules, reorganization of pigment particles, etc. which are crucial for living organisms depend on the active transport [3-6]. Biomolecular motors and their associated protein filaments together comprise an active transport system in living organisms that works by consuming energy obtained from hydrolysis of adenosine triphosphate (ATP) as fuel [7]. Biomolecular motors are tiny natural machines capable of converting chemical energy of ATP hydrolysis into mechanical work with a remarkably high energy efficiency and specific power [8]. The associated protein filaments serve as a track along which the biomolecular motors carry cargoes to various locations within a cell. Kinesin is a well-studied biomolecular motor that moves along microtubules (MTs) by consuming ATP [9]. MTs are hollow cylindrical protein filaments that are formed via polymerization of tubulin heterodimers [10]. Owing to the attractive features of biomolecular motor proteins such as nanometer scale, high fuel efficiency, engineering properties, etc. they have been considered promising candidates as building blocks and actuators in hybrid nanomechanical devices [11-13]. In vitro motility assay, where associated protein filaments are propelled on a substrate by surface-adhered motors proteins in the presence of ATP, has provided valuable insights into important aspects of biomolecular motor functions [14-16]. Based on the in vitro motility assay the MTs-kinesin system has been employed in synthetic environments for nanotransportation and nano-structuring [17,18], surface imaging [19], characterization of surface mechanical deformation [20], force measurement [21], etc. Very recently, molecular swarm robots have been fabricated based on an in vitro motility assay by combining MT-kinesin system with DNA [22]. While the MT-kinesin system has been receiving growing attention, the ability to control

motor function at the molecular level and motion of MTs in an in vitro motility assay is becoming essential for controlling the functions of integrated, hybrid biomolecular nanodevices. Various efforts have been documented in literature that aimed at controlling the functions of biomolecular motors in vitro by employing genetic engineering [23,24], azobenzene-based photo-switches [25], or tuning physico-chemical parameters, etc. [26]. In this work, we demonstrate a new strategy to reversibly control motility of MTs in an in vitro motility assay using a natural osmolyte trimethylamine-*N*-oxide (TMAO). We show that without sacrificing the concentration of fuel in the motility assay system the gliding velocity of MTs can be regulated over a broad range using TMAO in a concentration dependent manner. Interestingly, the motility of MTs can be completely turned off using TMAO of a relatively high concentration (≥3 M) even in the presence of the fuel. The halted motility of MTs can be fully restored upon elimination of the TMAO. Repeated cycles of addition and elimination of TMAO (≥3 M) enables complete inhibition and reactivation of the motility of MTs in a sequential manner without sacrificing their velocity. This work offers a simple, rapid and robust method to temporally regulate the motility of MTs in an in vitro motility assay in a reversible fashion while maintaining a constant supply of fuel. The rapid, reversible and repeatable regulation of the motility of the biomolecular motor system MT-kinesin demonstrated in this work will foster nanotechnological applications of biomolecular motors, such as in nano-transportation or molecular robotics etc. [27].

2. Materials and Methods

2.1. Chemicals and buffers

TMAO and polyethylene glycol 1K (PEG1K) were purchased from Sigma-Aldrich and used without further purification. Bovine serum albumin (BSA), glycerol, ethylene glycol (EG), and polyethylene glycol 6K (PEG6K) were purchase from Wako Pure Chemical Industries, Ltd. BRB80 buffer contained 80 mM PIPES, 1 mM $MgCl_2$, and 1 mM EGTA. The pH of BRB80 buffer was adjusted to 6.8 using KOH. PEG1K solution was prepared by mixing PEG1K with BRB80 buffer at a prescribed weight/volume (w/v) ratio. For example, 2.5 g PEG1K was mixed with 10 mL of BRB80 to prepare 25% w/v solution. Solutions of other osmolytes (25% w/v) including BSA, glycerol, EG, PEG6K were also prepared in BRB80 as described above. All the BRB80-osmolyte imaging solutions contained 5 mM ATP, 1 mM DTT, 2 mM trolox, 1 mM $MgCl_2$, 10 μM taxol, 0.5 mg mL^{-1} casein, 4.5 mg mL^{-1} D-glucose, 50 U mL^{-1} glucose oxidase, 50 U mL^{-1} catalase.

2.2. Purification, labelling of tubulin and preparation of MTs

Tubulin was purified from fresh porcine brain using a high-concentration PIPES buffer (1 M PIPES, 20 mM EGTA, 10 mM $MgCl_2$; pH adjusted to 6.8 using KOH) according to a previous report [28]. Atto550-labelled tubulin (RT) was prepared using Atto550 NHS ester (ATTO-TEC, Gmbh) according to a standard technique [29]. The labeling ratio of fluorescence dye to tubulin was ~1.0 as determined from absorbance of tubulin at 280 nm and fluorescence dye at 554 nm. MTs were prepared by polymerizing a mixture of RT and non-labelled tubulin (WT) (RT:WT = 1:1; final tubulin concentration = 40 μM). 4.0 μL of a mixture of RT and WT was mixed with 1 μL of GTP-premix (5 mM GTP, 20 mM $MgCl_2$, 25% DMSO in BRB80) and incubated

at 37 °C for 30 min. After polymerization the MTs were stabilized using paclitaxel (50 μM paclitaxel in DMSO).

2.3. Expression and purification of motor protein

GFP-fused recombinant kinesin-1 construct consisting of the first 465 amino acid residue of human kinesin-1 (K465), an N-terminal histidine tag, and a C-terminal Avidin-tag was used to propel MTs in an in vitro motility assay. The expression and purification of the kinesins were done as described in a previously published report [30].

2.4. In vitro motility assay

A flowcell with dimensions of 9×2×0.1 mm^3 (L×W×H) was assembled from two cover glasses (9×18) mm^2 and (40×50) mm^2 (MATSUNAMI) using a double-sided tape as a spacer. First, the flow cell was filled with 5 μL of 1 mg mL^{-1} streptavidin solution (Sigma-Aldrich, S4762) and incubated for 5 min. The flowcell was then washed with wash buffer (80 mM PIPES, 1 mM EGTA, 1 mM $MgCl_2$ and ~0.5 mg mL^{-1} casein; pH 6.8). Next 5 μL of K465 solution (800 nM) was introduced into the streptavidin coated flowcell. The flowcell was then incubated for 5 min to allow the binding of kinesins to the glass surface through interaction with streptavidin. After washing the flowcell with 10 μL of wash buffer, 10 μL of MT solution (200 nM, paclitaxel stabilized GTP-MTs) was introduced and incubated for 5 min, which was followed by washing with 10 μL of wash buffer. Finally, motility of MTs was initiated by applying 5 μL of motility buffer containing 5 mM ATP. In case of the experiments where TMAO was used, 5 μL of motility buffer containing 5 mM ATP and TMAO of prescribed concentrations was infused into the flowcell. The MTs were then monitored using a fluorescence microscope. The same method was used for other osmolytes tested. All the experiments using TMAO were performed at room temperature. The experiments in which various osmolytes were used at a concentration of 25% w/v (Supplementary Table-1) were performed at 20 °C.

2.5. Osmotic pressure and viscosity

Osmotic pressure values for PEG1K, PEG6K, BSA and TMAO were determined based on published data [31-33]. Osmotic pressure for glycerol and EG were calculated by $\pi = MRT$, where M is the molarity of the solution, R is the ideal gas constant, and T is the temperature in kelvin. Viscosity of osmolyte solutions were determined based on published data [34,35].

2.6. Repeated On/Off switching of the motility of MTs

Sequential inhibition (upon TMAO addition) and reactivation (upon TMAO wash out) of the motility of MTs was performed in a cyclic manner to test the ability to continuously switch the motility of MTs off and on. First motility of MTs was initiated by addition of motility buffer in the flowcell. The gliding MTs were monitored using an epi-fluorescence microscope. After 15 min period of motility of MTs in the presence of ATP, 3000 mM TMAO in ATP buffer was infused into the flowcell and incubated for an additional 15 min. The stationary MTs were monitored using an epi-fluorescence microscope. The TMAO buffer in the flowcell was replaced with motility buffer and the gliding MTs were monitored. This cycle was repeated for an additional three times. All these experiments were performed at room temperature.

2.7. Microscopy image capture and data analysis

Samples were illuminated with a 100 W mercury lamp and visualized by epi-fluorescence microscope (Eclipse Ti; Nikon) equipped with an oil-coupled Plan Apo 60×1.40 objective (Nikon). A filter block with UV-cut specification (TRITC: EX540/25, DM565, BA606/55; Nikon) was used in the optical path of the microscope that allowed visualization of MTs eliminating the UV part of radiation and minimized the harmful effect of UV radiation on samples. Images were captured using a cooled CMOS camera (Neo CMOS; Andor) connected to a PC. To capture images of MTs for several minutes, ND4 filter (25% transmittance) were inserted into the illuminating light path of the fluorescence microscope to avoid photobleaching.

All movies and images captured by the epi-fluorescence microscope were analyzed using an image analysis software (ImageJ 1.46r).

3. Results and discussion

3.1. TMAO-dependent suppression of motility of MTs

In this work we control the functions of a biomolecular motor system, MT-kinesin utilizing TMAO. In vitro motility assay has been a useful technique to investigate various biophysical and chemo-mechanical aspects of biomolecular motor protein systems. We employed in vitro motility assay of MTs on kinesins to explore utility of TMAO in controlling the functions of the MTs-kinesin. The in vitro motility assay of MTs was demonstrated on a kinesin coated substrate as represented schematically in Figure 1a. In brief, the surface of the motility assay substrate was first coated with streptavidin. K465 was attached to the substrate through interaction with the streptavidin. MTs were adsorbed to the kinesin coated substrate and motility of the MTs was initiated by supplying ATP (motility buffer) in the flowcell as the fuel. All the MTs exhibited gliding motion (100%) with an average velocity of 0.30±0.02 μm/s upon addition of the fuel (Figure 1b). TMAO is a natural osmolyte which is found in many eukaryotes [36,37] and is known for its stabilizing effect on protein structures [38]. TMAO has also been reported to modulate functions of various proteins and enzymes but the effect of TMAO is not universal to all proteins [39-41]. Recently, TMAO has been shown to stabilize MT filaments for an extended time period through inhibition of their depolymerization [34]. Nonetheless, there has been no report unveiling the effect of TMAO on the functions of MT-kinesin system. Therefore, it is intriguing to explore if TMAO has any effect on the functions of MTs and kinesins. TMAO of varying concentrations, ranging from 0 to 4000 mM, was employed in the motility assay by mixing with motility buffer in which the concentration of ATP was kept constant at 5 mM in each case. The effect of TMAO on the functions of MT-kinesins could be observed from a typical example of the motility behavior of a single MT during the gradual increment of TMAO concentration in motility buffer (Figure 2a). Supplementary movie 1 also shows gradual change in motility of MTs monitored at a fixed

field of view upon step-by-step increment of the concentration of TMAO in the motility buffer. In the presence of 750 mM TMAO the MTs exhibited gliding motion with an average velocity of 0.16±0.02 μm/s, which was 0.28±0.01 μm/s in the absence of the TMAO. The gliding velocity of MTs decreased further to 0.055±0.001 μm/s when TMAO concentration was increased to 1750 mM. Figure 2b shows overall change in velocity of MTs when concentration of TMAO was varied over a wide range (0-4000 mM). At relatively high TMAO concentration, e.g. 2500 mM the MTs still exhibited motility although the average velocity became much smaller (0.005±0.001 μm/s). Upon further increase of the TMAO concentration to 3000 mM or more, all the MTs (100%) completely lost their motility and remained stationary on the motility assay substrate despite the availability of the fuel (5 mM ATP) in the motility assay buffer. These results reveal that TMAO suppresses the activity of MT-kinesins as the result of which the velocity of kinesin-driven MTs in the in vitro motility assay decreased gradually with increasing the concentration of TMAO (Figure 2b). Surprisingly, TMAO at a relatively high concentration (3000 or more) completely terminated the motility of MTs on kinesins even though the fuel (ATP) was available in the motility buffer. These results demonstrate that the motility of MTs in an in vitro motility assay can be regulated over a wide range and can be even turned off simply by tuning the concentration of TMAO without changing the concentration of fuel or other physicochemical parameters.

3.2. Restoration of motility of MTs upon elimination of TMAO

Reversible regulation of functions of MT-kinesin is highly desired because of the prospective applications of this biomolecular motor system in nanotechnology. Therefore, we investigated the feasibility of restoring the TMAO-inhibited motility of MTs. Figure 3a shows motility behavior of a single gliding MT with time where the concentration of TMAO in motility assay buffer was gradually decreased from 1500 mM to 500 mM during the movement of the MT. Supplementary movie 2 also shows change in motility behavior of MTs upon decreasing the

concentration of TMAO gradually while the MTs were motile. As soon as the concentration of TMAO was decreased the MTs started to move with a higher velocity (Figure 3b). Sequential decrease in TMAO concentration and consequent increase in the velocity of MTs in the motility assay confirms that motility of MTs can be accelerated just simply eliminating the TMAO. This was also confirmed even using a concentration of TMAO higher than that used above (Figure 3). 1750 mM TMAO inhibited the motility of MTs and reduced their velocity from 0.31±0.01 μm/s to 0.056±0.002 μm/s. Upon elimination of the TMAO the MTs were found to regain their original velocity (0.30±0.01 μm/s) confirming the reversible regulation of the MT motility (Supplementary Figure 1). Collectively, based on the above results, it is evident that TMAO can be used to suppress MT motility and restoration of the motility can be realized upon elimination of TMAO. These results offer a simple means to reversibly regulate the motion of MTs in an in vitro motility assay.

3.3. Repeatability of the reversible regulation of MT motility

Next, we investigated whether the reversible regulation of the motility of MTs can be repeatedly demonstrated or not. We monitored behavior of motile MTs as a function of time in an in vitro motility assay in which the concentration of TMAO was repeatedly interchanged between 0 and 1000 mM. Figure 4a shows repeated change in the behavior of a motile MT as a function of time while the concentration of TMAO was repeatedly changed in the motility assay. The velocity of MTs was 0.28±0.01 μm/s in the absence of TMAO which decreased to 0.17±0.01 μm/s in the presence of 1000 mM TMAO. Upon removal of the TMAO by washing the velocity of the MTs was restored to 0.27±0.01 μm/s which is almost same to that observed in the absence of TMAO. This inhibition-restoration of the motility of MTs was repeatable for at least three cycles, as shown in the Figure 4b. These results confirm that using TMAO the regulation of MT motility can be demonstrated in a repeated manner for multiple cycles.

3.4. Repeated On/off switching of the motility of MTs

Finally, we sought to investigate whether the complete inhibition of the motility of MTs in the presence of high concentration of TMAO (≥3000 mM) is due to any permanent damage of MTs-kinesins caused by the TMAO or not. First, in an in vitro motility assay of MTs on kinesins we applied 3000 mM TMAO which rendered all the gliding MTs (100%) completely stationary (Figure 5a, 5b and 6a; Supplementary movie 3). We then replaced the TMAO in the flowcell by ATP buffer. Surprisingly, the MTs started gliding as soon as the TMAO in the flowcell was replaced by the ATP buffer (Figure 5c, Figure 6a and Supplementary movie 3). All the MTs (100%) resumed their motility with an average velocity of 0.27±0.02 μm/s, which is very close to that observed before termination of their motility by using TMAO 0.28±0.03 μm/s. Reactivation of the motility of MTs upon removal of the TMAO indicates that complete inhibition of the motility of MTs by TMAO was not the result of any permanent change or damage in kinesins and MTs. These results demonstrate an ability to temporally regulate motility of MTs in which high concentration TMAO can readily switch off the motility and elimination of the TMAO can again turn on the motility of MTs. Collectively these results demonstrate a simple, quick and efficient method for complete regulation of functions of MTs and kinesins in an in vitro motility assay through on/off switching of their activity. We further examined the repeatability of the on/off switching of MT motility using TMAO. Repeated cycles of TMAO addition (3000 mM TMAO in motility buffer) followed by removal were used to test the cyclic switching of the MT motility. In each cycle, motility buffer containing 3000 mM TMAO was infused into the flowcell and the kinesins and MTs remined inhibited for 15 min. The flowcell was then filled with motility buffer without TMAO to remove the TMAO from the flowcell. The motility of MTs was successfully turned off and switched on for at least 3 consecutive cycles upon addition and removal of TMAO respectively. All the MTs (100%) were deactivated and reactivated repeatedly within the cycles studied (Figure 6b). The number

of MTs bound per field of view (237.6×281.6 μm^2) was not noticeably changed by the cycling process (Figure 6c). Most importantly, no significant effect was also observed for the gliding velocity of MTs after each reactivation step within these three cycles (Figure 6d). Thus, the above experiments offer a simple, rapid and robust means to switch the motility of MTs on and off over multiple cycles with 100% MTs being transported and stopped.

In order to understand the mechanism behind inhibition of MT motility by TMAO, the ability of other osmolytes to induce similar effect was investigated using bovine serum albumin (BSA), glycerol, ethylene glycol (EG), polyethylene glycol1K (PEG1K, 1kDa molecular weight) and polyethylene glycol6K (PEG6K, 6kDa molecular weight). All the osmolytes were tested at a 25% w/v concentration. Among these osmolytes, only PEG1K, PEG6K and TMAO completely stopped the motility of MTs. The gliding velocity of MTs was 106±20 nm/s, 158±19 nm/s, 187±19 nm/s in the presence of BSA, glycerol, EG whereas that in the absence of the osmolytes was 313±35 nm/s. Although the velocity of MTs was decreased, BSA, glycerol, EG failed to completely inhibit the motility of MTs. Thus, we demonstrate that TMAO, as well as PEG, can completely inhibit the motility of MTs on kinesins in an in vitro gliding assay (Supplementary Figure 2). Collectively, all these observations could be accounted for by changes in the physicochemical properties of the solutions. Addition of osmolytes can change the viscosity, osmotic pressure, macromolecular crowding in solutions as shown in Supplementary Table-1. The motility of MTs on a kinesin coated substrate can be perturbed by changing the viscosity of the medium, although the extent of perturbation also depends on the kinesin density on the substrate [42]. However, in our work, any direct correlation between changes in the physicochemical properties of the solutions and inhibition/termination of MT motility is not obvious from the results. Both the TMAO and PEG are known for their kosmotropic behavior [43-46] i.e., promoting water structure and stabilizing proteins [47-49] and as discussed above both TMAO and PEG caused complete inhibition of the MT motility. Therefore, from the

above results it appears that the inhibition or termination of MT motility using TMAO might be correlated to a combination of the kosmotropic behavior and excluded volume/osmotic pressure effects associated with the osmolyte. TMAO is known for its stabilizing effects on proteins by virtue of these properties although the extent and consequence of stabilization varies depending on the proteins and enzymes [40,50]. With increasing concentrations of TMAO, proteins become more compact and their radius of gyration decrease [51]. As reported previously, excessive stabilization of heavy meromyosin structure by TMAO is linked to suppression of its enzymatic activity [52]. TMAO may have similar stabilizing effects on kinesins and consequently may cause inhibition of the ATPase activity of kinesins. The inhibition of the motility of MTs in the presence of TMAO reported in the present work might be associated to the inhibited activity of kinesins by TMAO. It is to note that, in case of PEG1K or PEG6K, the stopped motility of MTs was not resumed after washing of the flowcell as was done in case of TMAO. The reason is not clear at this moment for which further investigation is required in future.

In the past a significant amount of work has been reported in literature that attempted to control the motility of kinesin driven MTs in the in vitro gliding assay. Regulation of velocity of MTs has been realized by tuning temperature, or physicochemical parameters [26,53], but reversibility was not achieved. On the other hand, on/off switching of activity of the biomolecular motors was realized by regulating the availability of fuel either by uncaging ATP [54] or by buffer exchange [55]. Reversible switching of MT motility was achieved by using a thermo-responsive polymer surfaces, but this method caused desorption of MTs from the assay substrate [56]. Also, application of high temperature was a prerequisite which may affect the kinesins through thermal damage. Other methods involved engineering chemically regulated sites in kinesins [24] or oxidation/reduction of disulfide bonds in neck-linker region of engineered kinesins [57]. However, in these methods motility properties of kinesins were

affected by the engineering in the kinesins. Introduction of an allosteric-zinc binding site in F1-ATPase was successful in controlling this motor without impacting its activity [23]. Reversible inhibition of motor activity was demonstrated through sequential addition and chelation of Zn2p [58]. Such a binding on/off switch was effective in controlling activity of mutant kinesins, but the MT-binding affinity was greatly affected by the introduction of the zinc switch. Azobenzene-based photo-switches facilitated efficient photo-regulation of the biomolecular motors [25] but the gliding velocity of MTs could not be completely terminated in some instances. The present work for the first time introduces a method of utilization of a natural osmolyte which not only facilitates regulation of velocity of MTs but also permits complete on/off switching of the activity of MT-kinesins in a repeatable manner simply by tuning the concentration of TMAO. From the results of motility assay at different TMAO concentrations we noticed no adverse effect of TMAO on the binding between kinesins and MTs even in the 'off state' of the motility assay. Moreover, our method does not require regulation of fuel concentration or other physico-chemical parameters which probably will be advantageous for operation of bio-nanodevices with a range of different proteins in a combination and ATP-dependent processes for biosensing or fundamental biophysical studies.

4. Conclusions

In conclusion, we have described a new approach for regulating the motility of a nano-biomolecular machine MT-kinesin in vitro using a natural osmolyte TMAO. We are able to reversibly regulate the motility of MTs on kinesins using TMAO in a concentration dependent manner. Moreover, we have successfully demonstrated turning off and switching on the motility of the MTs in a repeated manner through cyclic application and removal of TMAO at relatively high concentration. This work offers a simple, rapid and robust method that enables repeated and reversible temporal regulation of the functions of kinesins/MTs without relying

on the regulation of concentration of fuel, cofactor composition or related physicochemical parameters. In this study, utilization of TMAO and tuning of its concentration for regulating activity of MTs-kinesins was demonstrated manually by exchanging buffer. A combination of this method with technology to precisely control the position of application of TMAO e.g., microfluidics, should enable both the spatial and temporal control over the activity of MT-kinesins. Nowadays biomolecular motors have been finding applications as actuators as well as sensors in integrated nanodevices, molecular robotics, etc. [22,59-60]. Therefore, such an ability to control activity of biomolecular motors at the molecular level as demonstrated in this work will greatly contribute to widen the applications of biomolecular motors in nanotechnology. At the same time, this work will motivate further exploration on the role of TMAO and other natural osmolytes in regulating the functions of biomolecular motors and other proteins in living organisms [40,61-62].

Acknowledgements

This work was financially supported by a research grant from Hirose International Scholarship Foundation, Japan (PK22181027) to A.M.R.K.; Future AI and Robot Technology Research and Development Project from New Energy and Industrial Technology Development Organization (NEDO), Japan; Grant-in-Aid for Scientific Research on Innovative Areas "Molecular Engine: Design of Autonomous Functions through Energy Conversion" (18H05423), Grant-in-Aid for Scientific Research (A) (18H03673) to A.K. from the Ministry of Education, Culture, Sports, Science and Technology, Japan.

Declaration of Competing Interest

The authors declare no competing financial interest.

References:

[1] Phillips, R.; Kondev, J.; Theriot, J. in *Physical Biology of the Cell*, Garland Science, 2009, NY, USA.

[2] Alberts, B.; Bray, D.; Watson, J.; Lewis, J.; Roberts, K.; Raff, M. in *Molecular Biology of the Cell*, Garland Science, 2012, 5th Edition, USA.

[3] Steinberg, G. *Trends Microbiol*., 2000, 8, 162-168.

[4] Vale, R. D. *Trends Biochem. Sci*, 1999, 24, M38-M42.

[5] Maniak, M. *Curr. Biol.*, 2003, 2, R917-R919.

[6] Klopfenstein, D. R.; Vale, R. D. *Mol. Biol. Cell*, 2004, 15, 3729-3739.

[7] Vale, R. D.; Fletterick, R. J. *Annual review of cell and developmental biology*, 1997, 13, 745-777.

[8] Howard, J. in *Mechanics of motor protein and cytoskeleton*, 2001, Sinauer Associates Inc.

[9] Yildiz, A.; Tomishige, M.; Vale, R. D.; Selvin, P. R. *Science*, 2004, 303, 676-678.

[10] Kirschner, M.; Mitchison, T. *Cell*, 1986, 45, 329-342.

[11] Van den Heuvel, M. G.; Dekker, C. S*cience*, 2007, 317, 333-336.

[12] Jia, Y.; Li, J. *Acc. Chem. Res.* 2019, 52, 1623-1631.

[13] Hess, H. *Annual review of biomedical engineering*, 2011, 13, 429-450.

[14] Harada, Y.; Noguchi, A.; Kishino, A.; Yanagida, T. *Nature*, 1987, 326, 805-808.

[15] Toyoshima, Y.; Kron, S. J.; Spudich, J. A. *Proc. Natl. Acad. Sci. U.S.A.*; 1990, 87, 7130-7134.

[16] Uyeda, T. Q.; Abramson, P. D.; Spudich, J. A. *Proc. Natl. Acad. Sci. U.S.A.* 1996, 93, 4459-4464.

[17] Bachand, G. D.; Rivera, S. B.; Boal, A. K.; Gaudioso, J.; Liu, J.; Bunker, B. C. *Nano Letters*, 2004, 4, 817-821.

[18] Bachand, G. D., Rivera, S. B., Carroll-Portillo, A., Hess, H.; Bachand, M. *Small*, 2006, 2, 381-385.

[19] Hess, H., Clemmens, J., Howard, J.; Vogel, V. *Nano Letters*, 2002, 2, 113-116.

[20] Inoue, D.; Nitta, T.; Kabir, A. M. R.; Sada, K.; Gong, J. P.; Konagaya, A.; Kakugo, A. *Nature Communications*, 2016 7, 12557.

[21] Hess, H.; Howard, J.; Vogel, V. *Nano Letters*, 2002, 2, 1113-1115.

[22] Keya, J. J.; Suzuki, R.; Kabir, A. M. R.; Inoue, D.; Asanuma, H.; Sada, K.; Hess, H.; Kuzuya, A.; Kakugo, A. *Nature Communications*, 2018, 9, 453.

[23] Liu, H.; Schmidt, J. J.; Bachand, G. D.; Rizk, S. S.; Looger, L. L.; Hellinga, H. W.; Montemagno, C. D. *Nature Materials*, 2002, 1, 173-177.

[24] Konishi, K.; Uyeda, T. Q.; Kubo, T. *FEBS Letters*, 2003, 580, 3589-3594.

[25] Amrutha, A. S.; Sunil Kumar, K. R.; Tamaoki, N. *ChemPhotoChem*, 2019, 3, 337-346.

[26] Böhm, K. J.; Stracke, R.; Unger, E. *Cell Biology International*, 2000, 24, 335-341.

[27] Sato, Y.; Hiratsuka, Y.; Kawamata, I.; Murata, S.; Nomura, S. I. M. *Sci. Robot.*, 2017, 2, eaal3735.

[28] Castoldi, M.; Popov, A. V. *Protein Expression and Purification*, 2003, 32, 83-88.

[29] Peloquin, J.; Komarova, Y.; Borisy, G. *Nature Methods*, 2005, 2, 299-303.

[30] Fujimoto, K.; Kitamura, M.; Yokokawa, M.; Kanno, I.; Kotera, H.; Yokokawa, R. *ACS NANO*, 2012, 7, 447-455.

[31] Canchi, D. R.; Jayasimha, P.; Rau, D. C.; Makhatadze, G. I.; Garcia, A. E. *J. Phys. Chem. B*, 2012, 116, 12095-12104.

[32] Vilker, V. L.; Colton, C. K.; Smith, K. A. *J. Colloid Interface Sci.*, 1981, 79, 548−566.

[33] Money, N. P.; *Plant Physiol.*, 1989, 91, 766-769.

[34] Bachand, G. D.; Jain, R.; Ko, R.; Bouxsein, N. F.; VanDelinder, V.; *Biomacromolecules*, 2018, 19, 2401-2408.

[35] Mei, L. H.; Lin, D. Q.; Zhu, Z. Q.; Han, Z. X. *J. Chem. Eng. Data*, 1995, 40, 1168-1171.

[36] Yancey, P. H.; Clark, M. E.; Hand, S. C.; Bowlus, R. D.; Somero, G. N. *Science*, 1982, 217, 1214-1222.

[37] Lidbury, I.; Murrell, J. C.; Chen, Y. *Proc. Natl. Acad. Sci. U. S. A.*, 2014, 111, 2710-2715.

[38] Zou, Q.; Bennion, B. J.; Daggett, V.; Murphy, K. P. *J. Am. Chem. Soc.*, 2002, 124, 1192-1202.

[39] Mashino, T.; Fridovich, I. *Arch. Biochem. Biophys.*, 1987, 258, 356-360.

[40] Kumar, R.; Serrette, J. M.; Thompson, E. B. *Arch. Biochem. Biophys.*, 2005, 436, 78-82.

[41] Rani, A.; Jayaraj, A.; Jayaram, B.; Pannuru, V. *Sci. Rep.*, 2016, 6, 23656.

[42] Hunt, A. J.; Gittes, F.; Howard, J. *Biophysics. J.*, 1994, 67, 766-781.

[43] Sackett, D. L. *Am. J. Physiol.*, 1997, 273, R669-676.

[44] Schummel, P. H.; Gao, M.; Winter, R. *ChemPhysChem* 2017, 18, 189-197.

[45] Chen, W. Y.; Hsu, M. Y.; Tsai, C. W.; Chang, Y.; Ruaan, R. C.; Kao, W. H.; Huang, E. W.; Chung Chuan, H. Y. T. *Langmuir*, 2013, 29, 4259-4265.

[46] Liao, Y.T.; Manson, A. C.; DeLyser, M. R.; Noid, W. G.; Cremer, P. S. *Proc. Natl. Acad. Sci. U. S. A.* 2017, 114, 2479-2484.

[47] Ma, J., Pazos, I. M.; Gai, F. *Proc. Natl. Acad. Sci. U. S. A.*, 2014, 111, 8476-8481.

[48] Moelbert, S.; Normand, B.; De Los Rios, P. Biophys. Chem., 2004, 112, 45-57.

[49] Kane, R. S.; Deschatelets, P.; Whitesides, G. M. *Langmuir*, 2003, 19, 2388-2391.

[50] Yancey, P. H. *J. Exp. Biol.*, 2005, 208, 2819-2830.

[51] Hilaire, M. R.; Abaskharon, R. M. and Gai, F.J. Phys. Chem. Lett., 2015, 6, 2546-2553.

[52] Kumemoto, R.; Yusa, K.; Shibayama, T.; Hatori, K. *Biochimica et Biophysica Acta (BBA)-General Subjects*, 2012, 1820, 1597-1604.

[53] Kawaguchi, K; Ishiwata, S. *Cell Motil. Cytoskeleton*, 2001, 49, 41-47.

[54] Hess, H.; Clemmens, J.; Qin, D., Howard, J.; Vogel, V. *Nano Lett.*, 2001, 1, 235-239.

[55] Bohm, K. J.; Stracke, R.; Baum, M.; Zieren, M.; Unger, E. *FEBS Lett.*, 2000, 466, 59-62.

[56] Lonov, L.; Stamm, M.; Diez, S. *Nano Lett.*, 2006, 6, 1982-1987.

[57] Tomishige, M.; Vale, R. D.; J Cell Biol., 2000, 151, 1081-1092.

[58] Greene, A. C.; Trent, A. M.; Bachand, G. D. *Biotechnol and Bioengineering*, 2008, 101, 478-486.

[59] Matsuda, K.; Kabir, A. M. R.; Akamatsu, N.; Saito, A.; Ishikawa, S.; Matsuyama, T.;

Ditzer, O.; Islam, M. S.; Ohya, Y.; Sada, K. and Konagaya, A. *Nano Lett.,* 2019, 19, 3933-3938.

[60] Hagiya, M.; Konagaya, A.; Kobayashi, S.; Saito, H.; Murata, S. *Accounts of Chemical Research*, 2014, 47, 1681-1690.

[61] Burg, M. B.; Ferraris, J. D. *Journal of Biol. Chem.*, 2008, 283, 7309-7313.

[62] Nadel, C. M.; Mackie, T. D.; Gardner, R. G. *PLoS Genetics*, 2019, 15, e1008115.

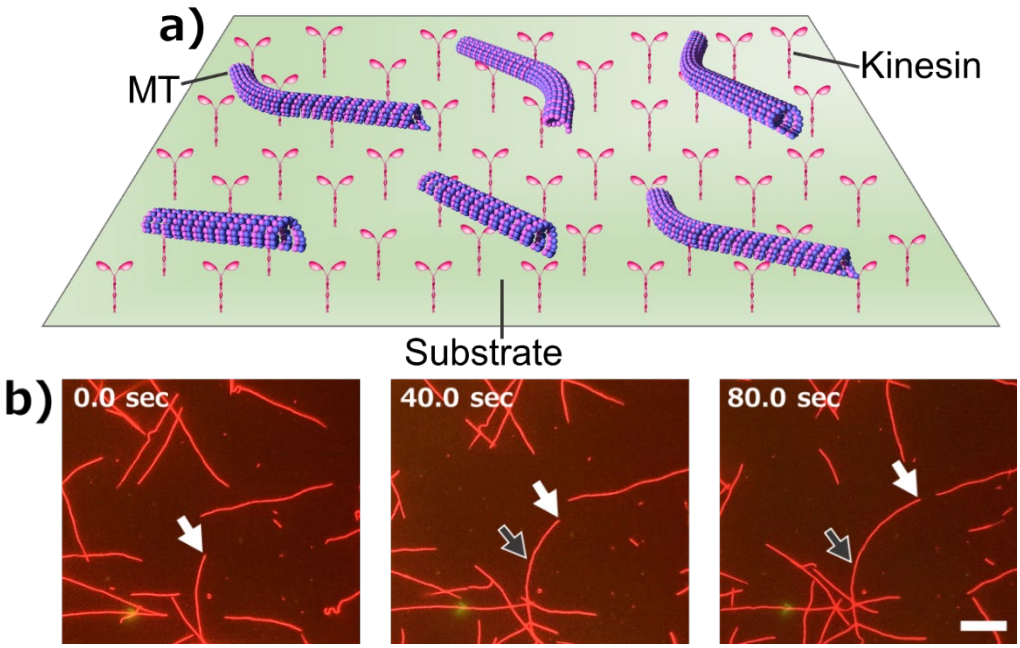

Figure 1: (a) Schematic illustration of an in vitro motility assay of MTs on a kinesin-coated substrate. (b) Time lapse fluorescence microscopy images show motility of MTs on the kinesin-coated substrate in the in vitro motility assay. The white arrowheads indicate position of the leading end of a gliding MT. The black arrowheads indicate original position of the leading end of the MT. Scale bar: 10 µm.

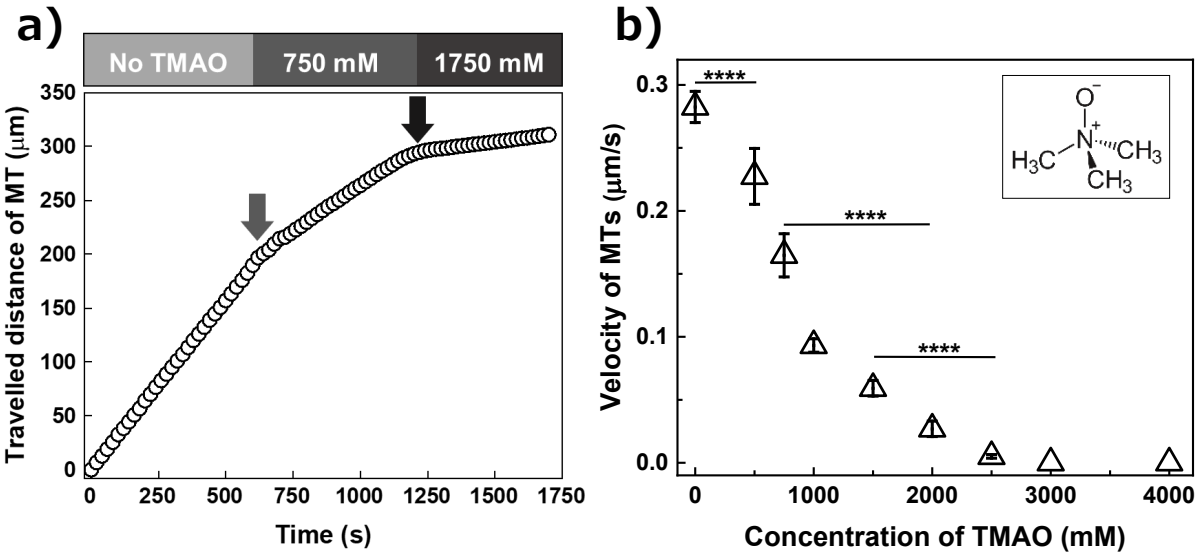

Figure 2: Suppression of motility of kinesin-driven MTs in an in vitro motility assay using TMAO. (a) Behavior of a single MT upon sequentially increasing the concentration of TMAO in the motility assay buffer. Plotted is the travelled distance of one MT as a function of time. The travelled distance was determined by manually tracking the trailing end of the MT. The arrowheads indicate starting point where motility behavior of the MT was changed due to the change in concentration of TMAO in the motility assay buffer. The upper panel shows the corresponding concentration of TMAO in the motility assay. (b) Change in average gliding velocity of MTs upon increasing the concentration of TMAO in motility assay buffer. The velocity of MTs gradually decreased upon increasing TMAO concentration and motility was completely halted at relatively high TMAO concentration (3000 mM). Further increase in TMAO concentration to 4000 mM brought no change for the stationary MTs. Statistical analysis according to Student's t-test confirmed significant difference, indicated by ****, among the velocities of MTs at different conditions ($P<0.0001$). Inset shows the chemical structure of TMAO. Error bars: standard deviation.

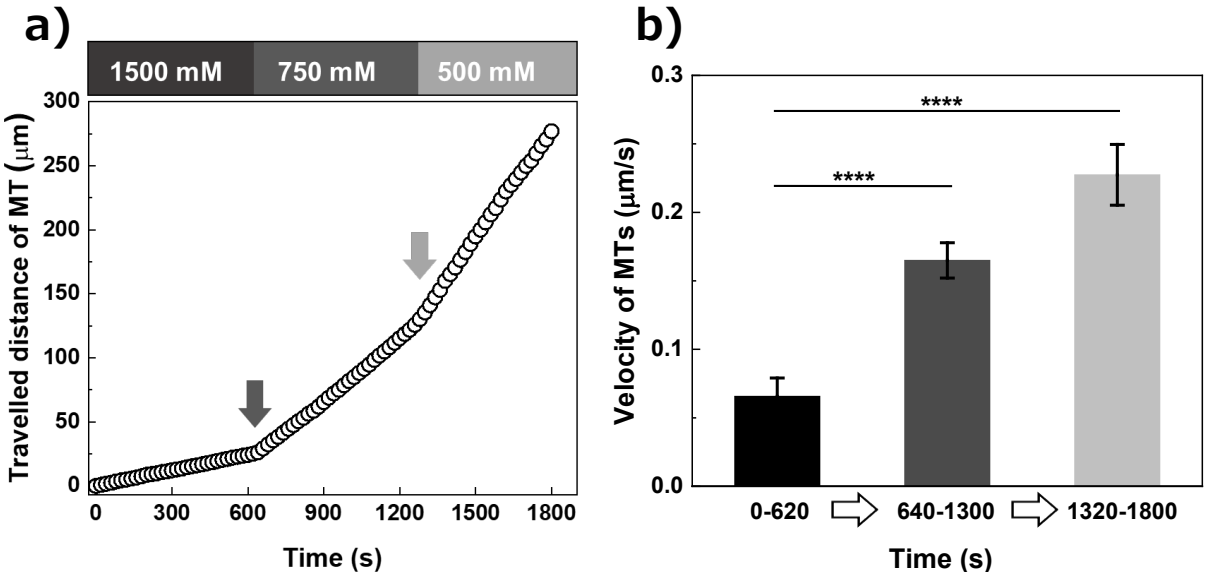

Figure 3: Acceleration of motility of kinesin-driven MTs in an in vitro motility assay upon decreasing the concentration of TMAO in the motility assay buffer. (a) Behavior of a single MT upon sequentially decreasing the concentration of TMAO in the motility assay buffer. Plotted is the travelled distance of one MT as a function of time. The travelled distance was determined by manually tracking the trailing end of the MT. The arrowheads indicate starting point where motility behavior of the MT was changed due to the change in concentration of TMAO in the motility assay buffer. The upper panel shows corresponding concentration of TMAO in the motility assay. (b) Change in average velocity of MTs at different time ranges due to the decrease in concentration of TMAO in the motility assay buffer. The time ranges 0-620 s, 640-1300 s, and 1320-1800 s correspond to the presence of 1500, 750 and 500 mM TMAO in the motility assay respectively. The velocity of MTs gradually increased upon decreasing TMAO concentration. Statistical analysis according to Student's t-test confirmed significant difference, indicated by ****, among the velocities of MTs at three different conditions ($P<0.0001$). Error bars: standard deviation.

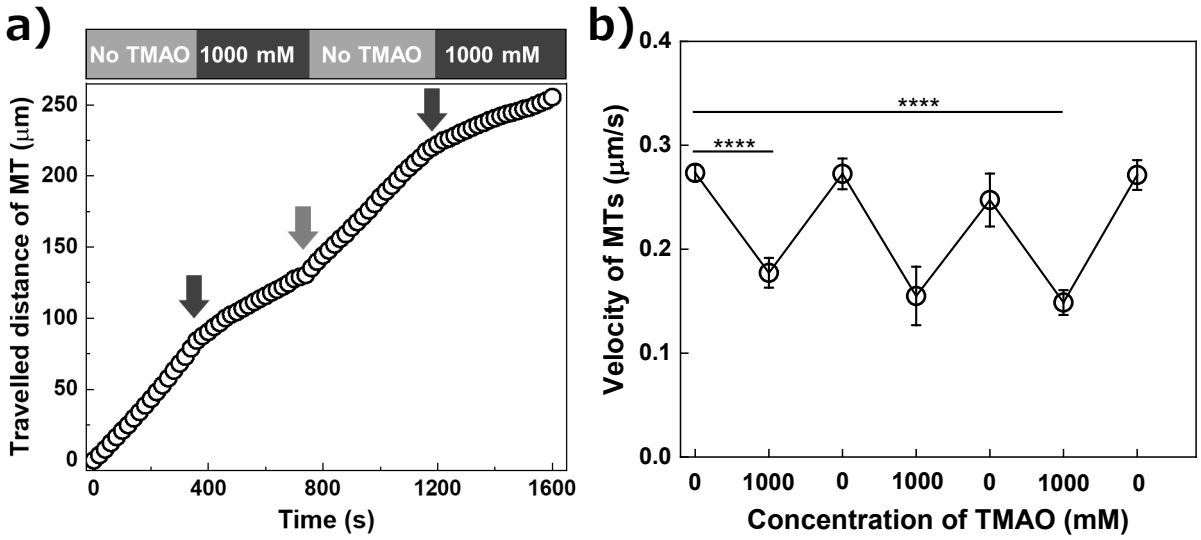

Figure 4: Repeated change in motility of kinesin-driven MTs in an in vitro motility assay upon cyclically changing the concentration of TMAO. (a) Motility behavior of a single MT upon sequentially changing the concentration of TMAO in the motility assay buffer between 0 and 1000 mM. Plotted is the travelled distance of one MT as a function of time. The travelled distance was determined by manually tracking the trailing end of the MT. The arrowheads indicate starting point where motility behavior of the MT was changed due to the change in concentration of TMAO in the motility assay buffer. The upper panel shows corresponding concentration of TMAO in the motility assay. (b) Change in average velocity of MTs upon cyclically changing the concentration of TMAO in the motility assay buffer between 0 and 1000 mM. Statistical analysis according to Student's t-test confirmed significant difference, indicated by ****, among the velocities of MTs at different conditions ($P<0.0001$). Error bars: standard deviation.

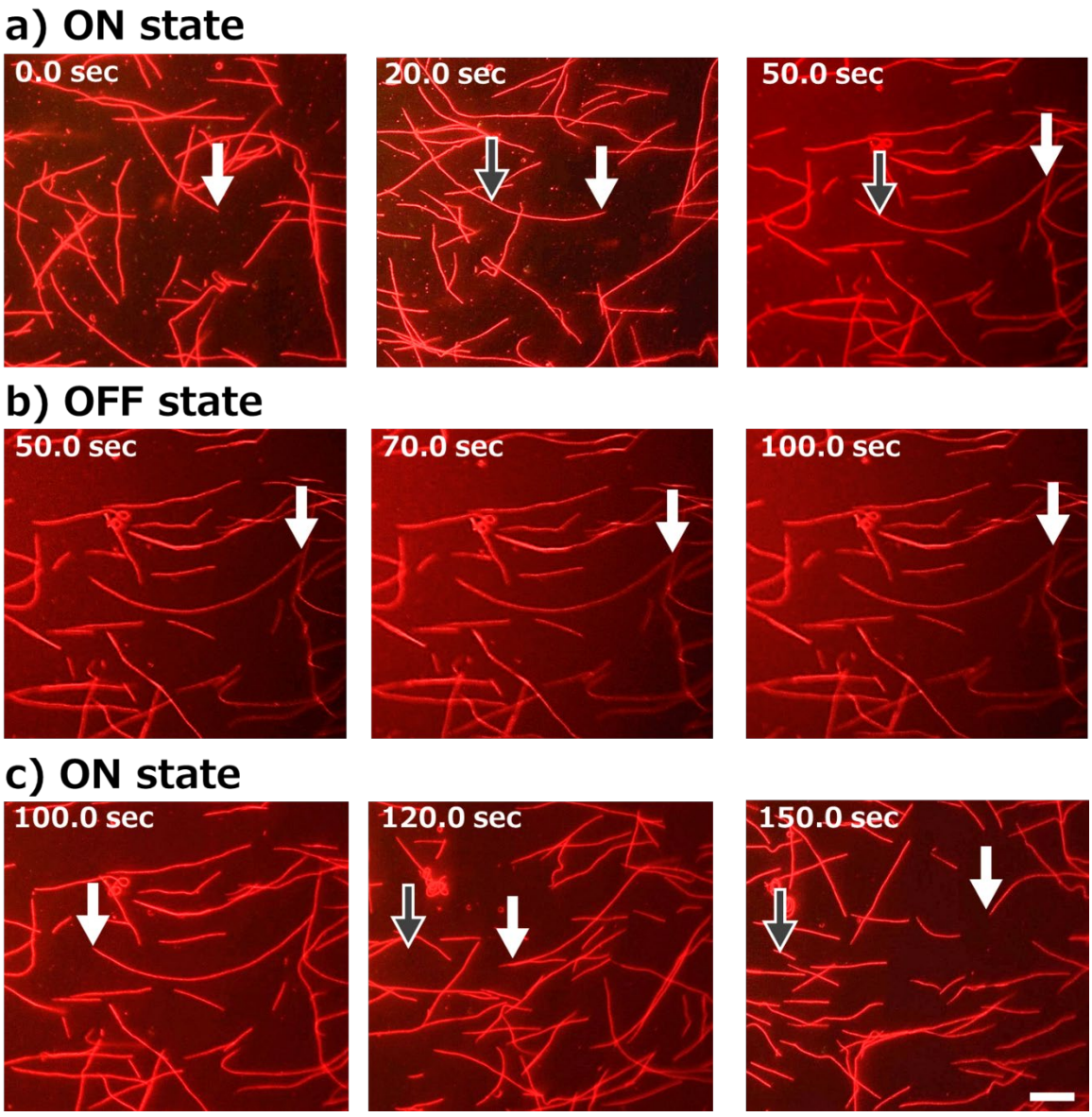

Figure 5: Time-lapse fluorescence microscopy images showing on/off switching of the motility of MTs using TMAO (3M). The MTs were motile in the absence of TMAO (ON state). Motility of the MTs was completely halted (OFF state) in presence of TMAO (3000 mM) despite the presence of ATP in the motility assay buffer. The motility of MTs was restored upon removal of the TMAO (ON state). The white arrowheads in 'a' indicate position of the leading end of a gliding MT. In 'b', the white arrowheads indicate the same end of that MT which was gliding in 'a' but stationary in 'b'. In 'c', the white arrowheads indicate the trailing end of a gliding MT. The black arrowheads indicate original position of the leading end and trailing end of a MT in 'a' and 'c' respectively. Scale bar: 10 µm.

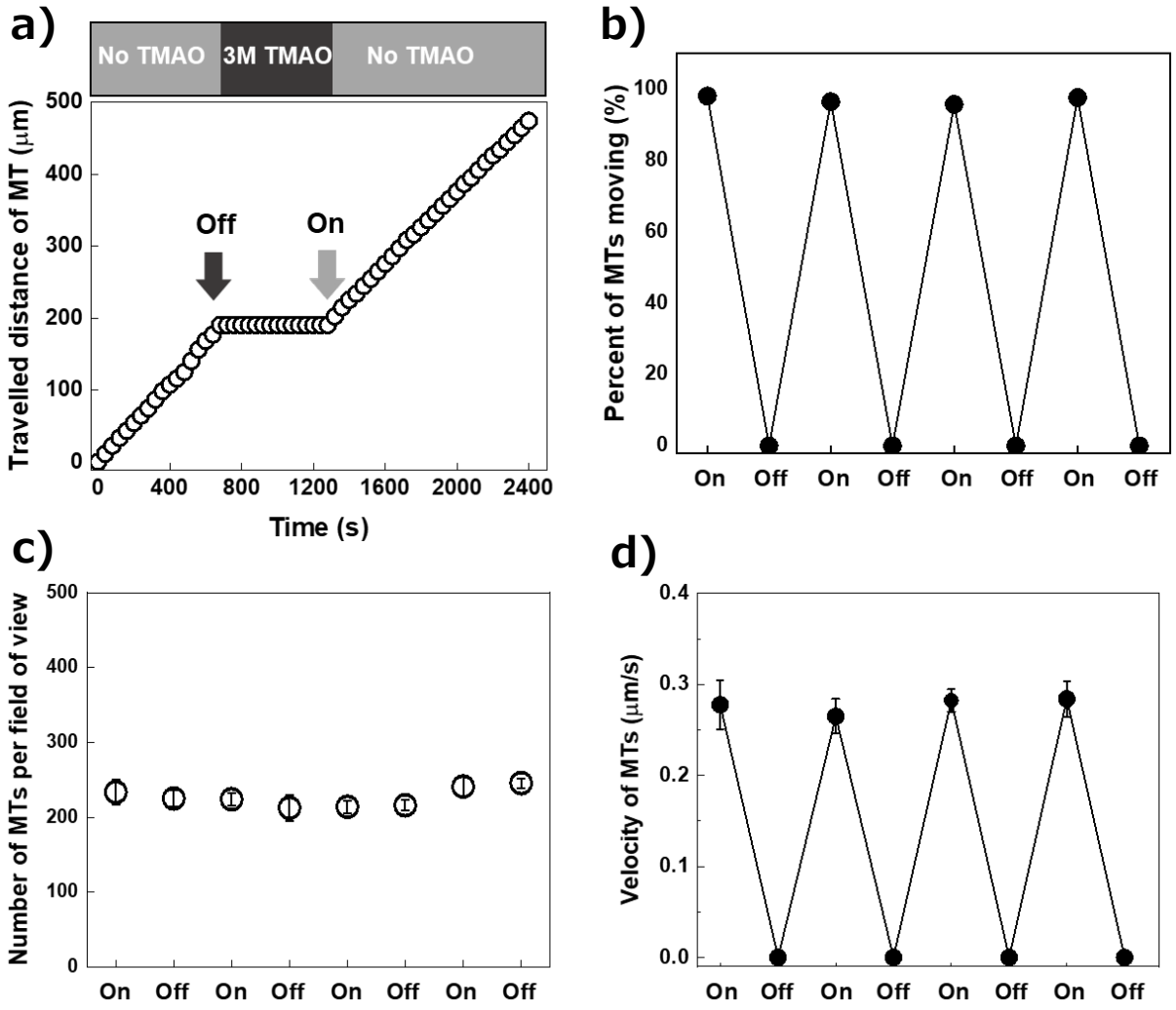

Figure 6: On/off switching of the motility of MTs using TMAO (3 M). (a) Motility behavior of a single MT in the absence and in the presence of 3 M TMAO. Plotted is the travelled distance of one MT as a function of time. The travelled distance was determined by manually tracking the trailing end of the MT. The arrowheads indicate starting point where motility behavior of the MT was changed due to the change in concentration of TMAO in the motility assay buffer. The upper panel shows corresponding concentration of TMAO in the motility assay. (b) Change in percentage of MTs moving, (c) average number of MTs per field of view, and (d) velocity of MTs upon changing the concentration of TMAO cyclically between 0 and 3 M. Here, 'Off' and 'On' refer to presence of 3M TMAO and absence of TMAO in the motility assay that resulted in 'stationary' and 'mobile' state of MTs respectively. Error bars: standard deviation.